# Analysis of Lossy Mode Resonance Sensing System Using Measurement Uncertainty of Type A

## Yu-Cheng Lin\*

Department of Electronic Engineering, Ming Chuan University

#### **ABSTRACT**

This paper for the first time presents the measurement uncertainty evaluation of type A for a lossy mode resonance (LMR) sensing system. The LMR sensor consists of an Indium Tin Oxide (ITO) thin-film coated on glass. The analysis of measurement uncertainty for the light source, the platform, and the LMR sensor is carried out. As a result, based on the condition of a 95% confidence level for the LMR sensing system, the uncertainty of LMR wavelength of 0.43 nm was obtained and the uncertainty of LMR transmission was shown to be 0.0289. The proposed methodology could be applied to other sensing systems to improve the measurement precision and raise the confidence level.

**Keywords:** Indium Tin Oxide, confidence level, optical spectrum, refractive index

# 以A類量測不確定性分析損耗模態共振感測系統

林鈺城\*

銘傳大學電子工程學系

## 摘 要

本文首次提出了損耗模式共振式(LMR)感測系統的 A 型測量不確定度評估。LMR 感測器是由鍍在玻璃上的氧化銦錫(ITO)薄膜組成。研究中,針對光源和 LMR 感測平台的量測不確定度進行了分析,結果在 95%的信心水準條件下,得到 LMR 波長的不確定度為 0.43nm,LMR 穿透度的不確定度為 0.0289。本研究所提出的不確定度估算方法,也可以應用於其他感測系統,以提高測量精度並提高不確定度的信心水準。

關鍵詞:氧化銦錫、信心水準、光譜、折射率

文稿收件日期 110.10.20; 文稿修正後接受日期 111.1.27; \*通訊作者

#### I. INTRODUCTION

Understanding environmental information is necessary for the correct detection of essential factors that may be classified into physical parameters such as temperature, pressure, humidity, and biological characteristics, which especially important for determining concentrations of contaminants, cells, and viruses[1]. Over the years, optical sensors have become an attractive topic for researchers in many applications due to their benefits such as compact size, low weight, electromagnetic protection, and high sensitivity. Thin-film coating onto optical waveguides with metallic materials has become a widely explored technique in the field of sensors. The most wellknown phenomenon is Kretschmann structurebased surface plasmon resonance (SPR), which has been extensively studied because of its many applications ranging from biomaterials inspection, chemical detection, [2-4] and physical testing [5, 61.

Another widely studied optical sensing system is based on the lossy mode resonance (LMR) principle. Using the Kretschmann structure, the metal layer in SPR is replaced with a semiconductor film material of a specific thickness. If the phase-matching condition is met and the mode fields between the waveguide and thin-film overlap a lot, the waveguide mode is transmitted to the film material. A great energy loss occurs and this phenomenon is called LMR [7]. Compared with the SPR principle, LMR materials are for materials whose real part of the dielectric constant is positive and greater than the imaginary part; and the real part of its dielectric constant must also be greater than the ambient dielectric constant. The sensitivity of LMR elements can generally reach 4000-5000 nm/RIU, which is equivalent to the best sensitivity of SPR, but Francisco et al. once achieved sensitivity of 20,000 nm/RIU [8], far exceeding SPR. In addition, the numbers of peaks and valleys are not only one. As the thickness of the thin film dielectric material increases, the number of peaks and valleys increases accordingly. LMR is different when testing external substances, and the positions of its loss peaks and valleys move.

Therefore, sensing of humidity [9], gas [10], acid, alkali [11, 12], and biological materials [13-15] has been carried out. Most of the current LMR element structures use optical fibers as the light guide substrate. Among the optical waveguide materials, optical fibers have the advantages of being light-weight, and anti-static, as well as enabling multi-tasking, and anti-electromagnetic interference. However, the diameter of glass optical fibers is about 125 µm, which results in a fragile structure. The length of about 1 meter, called the leading fiber, must be reserved for connecting during measurement or installation. The process of coating and surface modification of the entire fiber sensing element becomes more difficult owing to the leading fiber. It is extremely unfavorable for mass production. This is a big problem for sensor production in the future. Therefore, planar glass as a waveguide substrate has been proposed to develop an LMR sensor to detect different refractive indexes of the analyte [16-18]. The planar structure offers a more robust platform than optical fiber. Therefore, the slab waveguide setup is easier to handle. Another important advantage with the planar waveguide is that it is possible to operate in a wide spectrum with either TE or TM resonance. In addition, the waveguide can be deposited on both sides, making it easy to obtain a two-parameter sensor or even a two-channel microfluidic system.

The LMR sensor is one of the sensing technologies with great development potential in the field of biomedicine. The problem in biosensing is the standardization of measurement. Because of the dynamic interaction biomolecules and the non-uniform distribution of the analytes, the reaction can only reach an equilibrium state, not a static state. This results in great measurement uncertainty. The requirements of precision and accuracy for the detection of biomolecules are extremely high, and the measurement error or uncertainty is relatively important. However, in the current published research literature about neither SPR nor LMR, the measurement uncertainty has not been discussed, even though it is very important.

Regarding measurement uncertainty, there is an international standard [19] to be followed. For a long time, error analysis has been a part of measurement science or metrology practice, and

it is also a concept that most engineers apply. Therefore, in the history of measurement development, uncertainty as a quantifiable concept is relatively new. It is now generally recognized that when all known or suspicious error components have been included in the assessment scope and appropriate corrections have been applied, there is still uncertainty regarding the correctness of the results. The measurement result represents the possible range of the true values of the measured quantity. In addition, in many industrial and commercial applications, as well as in the field of health and safety, it is usually necessary to provide a range of measurement results that contains most of the values that may be reasonably distributed. Therefore, an ideal method for evaluating and expressing measurement uncertainty must be proposed in such intervals, especially intervals with coverage probability or confidence levels.

In this paper, based on the specifications of ISO/IEC GUIDE 98-3:2008(E)[19], the Type A method is used to estimate the measurement uncertainty of the proposed LMR sensing platform. The second section explains the manufacturing process of the LMR sensor and the spectrum integration method. The third section shows the measurement uncertainty of the optical power intensity including for the light source and platform, and finally the LMR sensing system. The fourth section is the conclusion.

#### II. MATERIAL AND METHOD

#### 2.1 Spectrum measurement

The setup of the light source stability measurement system is shown on the top side of Fig. 1. A halogen white light (AQ4303B, ANDO Co. Ltd.) with 400~1800 nm wavelength worked as the input source and an optical spectrometer (USB 2000, Ocean Optics®) was used as the receiver to measure the spectrum of the sensor. An optical fiber patch-cord with an SMA connector and an FC connector (QP600-1-UV-VIS), which has a core diameter of 600 µm, and was purchased from Ocean Optics Co., was used to link the light source and the spectrometer that connect to the PC (personal computer) for spectrum data acquisition. The spectrum was

recorded every 5 seconds and the data acquisition was repeated 20 times.

A schematic giving the details of the experimental setup and the photograph of the LMR sensor held with the alignment bulk platform is also shown on the bottom side of Fig. 1. For easy self-alignment, the bulk platform was designed in advance to fit all components, and the optical axis was along the center of the LMR sensor. An optical fiber patchcord with an FC connector (M74L01) purchased from Thorlabs Co. Ltd., which has a core/cladding diameter of  $400/425~\mu m$  and NA 0.39, was inserted into the hole at the left side of the platform and the optical fiber patchcord (QP600-1-UV-VIS) was inserted into the right side for the spectrometer.

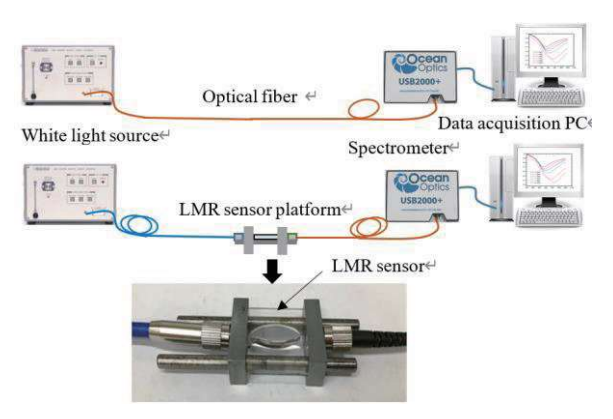


Fig. 1. A schematic of the experimental setup for light source spectrum and LMR sensor alignment bulk platform

#### 2.2 LMR sensor fabrication

LMRs are generated due to the guidance of a mode in the nanocoating deposited on optical glass waveguides. Before sputtering, all the sodalime glass sheets with 0.4 mm thickness, provided by Liefco Optical Inc. (Taichung, Taiwan), were pre-cleaned with acetone using purity wipes. The glass sheets were used as the substrate in a sputter coating process. The coating equipment was supplied by IZOVAC Co. The ITO target, composed of 90% In<sub>2</sub>O<sub>3</sub> and 10% SnO<sub>2</sub> with a purity of 3N to 4N, was purchased from Summit Tech. Co. Ltd. A detailed description of the coating process can be referenced in [20]. After sputtering, all the ITO glass sheets were cut into  $30 \times 30$  mm square sizes. The thickness of the ITO film was obtained at about 100 nm with an

optical interferometer instrument.

#### 2.3 Analyte material

The solutions with the different refractive indexes used to characterize the refractive response of the LMR sensor were prepared by adjusting the concentration of glycerol in water from 0% to 100% in steps of 20%. The glycerol was obtained from Huaho Chemical Co. (Taoyuan, Taiwan). The aqueous solutions were prepared with ultrapure water (> 18.2 M $\Omega$ -cm) by the Milli-Q system (Burlington, MA, USA). The refractive indices of samples were dropped on the prism surface and read with a handheld refractometer (R-5000, ATAGO Ltd. Co.).

#### 2.4 Measurement of uncertainty in Type A

Based on section 4.2 in the documentation of the uncertainty of measurement [19], the best available estimate of the expected value of a quantity q that varies randomly is the mean or average of the n observations for  $q_k$ , which is denoted as  $\overline{q}$  in eq.(1).

$$\overline{q} = \frac{1}{n} \sum_{k=1}^{n} q_k \tag{1}$$

The n independent observations  $q_k$  are obtained under the same conditions of measurement. The individual observations  $q_k$  disturb measurements randomly owing to random effects during measurement. The experimental variance  $s^2$  of the observations is denoted by eq.(2)

$$s^{2}(q_{k}) = \frac{1}{n-1} \sum_{j=1}^{n} (q_{j} - \overline{q})^{2}$$
 (2)

The terms  $s^2$  estimates the variance  $\sigma^2$  of the probability distribution of q. The positive square root  $s(q_k)$  is the experimental average standard deviation used to characterize the variability of the observed values  $q_k$ . The best estimate of the variance of the mean is given by

$$s^2(\overline{q}) = \frac{s^2(q_k)}{n} \tag{3}$$

The experimental average standard deviation of the mean  $s(\overline{q})$  is equal to the positive square root of  $s^2(\overline{q})$ . The  $s(\overline{q})$  also quantifies how well q estimates the expectation of q and is used as a measure of the uncertainty of q. The physical

mechanism is based on the power perturbation of the light source, photoelectric conversion efficiency, and thermal noise of electronic instruments, which cause random effects of measurement. The  $q_k$  represents each optical intensity for the light source measurement and is the resonance wavelength for each LMR measurement. The average standard deviation is regarded as the average offset value from the average for all the measurement results.

The standard uncertainty of y is denoted by u(y) where y is the estimate of the measurand Y and is the average standard deviation for the result of measurement. The additional measure of uncertainty provides an interval that can be termed as expanded uncertainty, denoted by U. The expanded uncertainty U is obtained by multiplying the standard uncertainty u (y) by a coverage factor k:

$$U = k \cdot u(y) \tag{4}$$

The result of a measurement is then conveniently expressed as  $Y = y \pm U$ . It indicates that the best estimate of the value related to the measurand Y is y. In other words, the interval from y - U to y + U is expected to cover a large fraction of the distribution of values attributed to Y.

The confidence interval and confidence level are two important terms with specific definitions in statistics. They apply to the interval defined by U. An expanded uncertainty with k is intended and the interval  $y - ku_c(y)$  to  $y + ku_c(y)$ has a specified level of confidence p associated with the normal distribution. For a normal distribution with expectation µ and standard deviation  $\sigma$ , the interval  $\mu \pm \sigma$  (k=1) covers approximately 66.27% of the distribution. Furthermore, the interval  $\mu \pm 2\sigma$  (k=2) and  $\mu \pm 3\sigma$ (k=3) encompass approximately 95.45% and respectively. 99.73%, In the uncertainty measurement estimation for the LMR sensor platform, k=2 is applied because the 95% confidence level is high enough to meet the requirement for normal measurement.

#### III. RESULTS

#### 3.1 Uncertainty for light source

The optical spectrum for the light source was recorded from 600 nm to 1100 nm and the mean (black square) and average standard deviation (red circle) are shown in Fig. 2. Along with the increase of the wavelength, the optical power intensity increases from 0.37 µW to 0.71 µW and then remains above 0.63 µW. The average intensity is 0.61 µW. The highest value of average standard deviation occurs at the wavelength of 608.5 nm  $(7.70 \times 10^{-4} \mu W)$  and the lowest value is at 1002.5 nm (1.92  $\times$  10<sup>-4</sup>  $\mu$ W). The average value is  $4.13 \times 10^{-4} \mu$ W. There is no obvious correlation between the average standard deviation and the power intensity. In other words, compared under different wavelength conditions, the spectrum of a light source with greater intensity will not produce a greater average standard deviation.

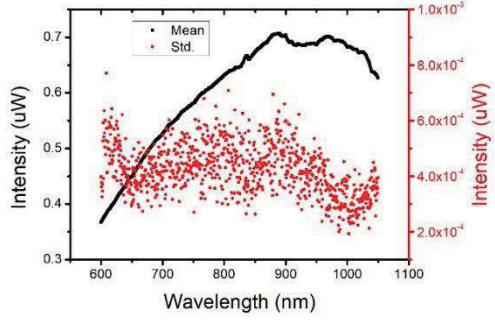


Fig. 2. The optical spectrum of the light source where the black squares represent the mean and the red circles are the distribution of average standard deviation

## 3.2 Uncertainty for the platform

During to the setting up for the LMR platform in Fig. 1, the spectrum was read 20 times for the surrounding air. The result is shown in Fig. 3. The maximum value of mean occurs at 675.5 nm ( $2.72 \times 10^{-2} \mu W$ ); the minimum value occurs at 1050.0 nm ( $1.77 \times 10^{-2} \mu W$ ); the average value is  $2.14 \times 10^{-2} \mu W$ . The highest value of average standard deviation ( $3.84 \times 10^{-4} \mu W$ ) is obtained at 610.0 nm, the lowest value ( $5.59 \times 10^{-5} \mu W$ ) is at 976.5 nm, and the average value is at  $1.72 \times 10^{-4} \mu W$ . The intensity of the light source drops significantly after passing through the LMR sensor. Because the LMR sensor is composed of soda-lime glass coated with an ITO film, the light source was

guided by an optical fiber and then coupled into this glass waveguide. The second optical fiber patchcord connecting to the output of the glass waveguide guided the light into the spectrometer. Some loss occurred during the light-guiding process. The first was the coupling loss between the optical fiber patchcord and the glass waveguide. The second was the absorption of the soda-lime glass. In the near infrared spectrum from 680 nm to 1000 nm, the transmission of the soda-lime glass decreased gradually [21]. The third loss occurred because the long-wavelength light cannot maintain total internal reflection (TIR). With the dispersion curve of soda-lime glass [22], the refractive index in the longwavelength spectrum gradually decreases, which causes the refractive index of the waveguide layer to approach that of the ITO film [23]. As a result, it was difficult for TIR to occur and greater loss happened, especially after the wavelength exceeded 840 nm. All the above losses are collectively referred to as component insertion loss (IL), which is defined as eq.(5).

$$IL = 10 \cdot \log(\frac{P_{platform}}{P_{light \, source}}) \tag{5}$$

The  $P_{platform}$  and  $P_{light\ source}$  are relative to the power intensity of LMR platform and light source.

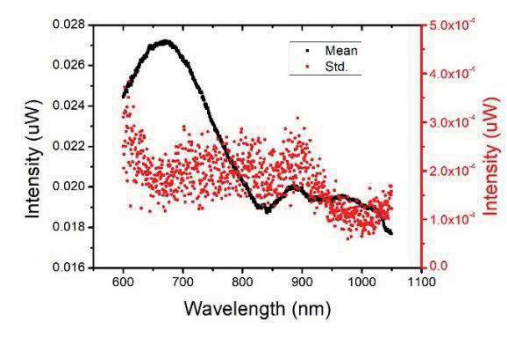


Fig. 3. The optical spectrum of the LMR platform where the black square represents the mean and the red circles are the distribution of average standard deviation

The *IL* spectrum of the LMR sensor platform is shown in Fig. 4. The *IL* for all wavelengths is below -11.8 dB. The proportion of short-wavelength loss is not high but the IL gradually decreases from -11.8 dB (600 nm) to -15.6 dB (840 nm). The *IL* stays at approximately -15.5 dB after a wavelength greater than 840 nm.

Such a descending curve is very similar to that in Fig. 3. This is because ITO materials have greater absorption for light greater than 840 nm.

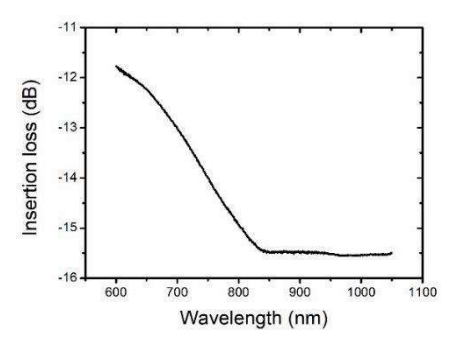


Fig. 4. The IL spectrum of the LMR sensor platform

Another issue worth discussing is whether the reduce of the average standard deviation for the light source is correlated to the reduce of the average light intensity. Therefore, the average value and the average standard deviation of the light source and the LMR platform are subtracted separately to observe the decreasing range of the average value, noted by diff. Mean, and the decrease range of the average standard deviation, noted by diff. Std. The result is shown in Fig. 5. The spectrum for the reduce in the average value (black square) is similar to that of the shape in Fig. 2, where the maximum value of 0.69 µW occurs at 882.5 nm. Comparing to different wavelengths, there is no positive correlation between the reduce in the average standard deviation (red circle) and the reduce in the average (black square). Although the light intensity of LMR is inherently much smaller than that of the light source, the average standard deviation is only slightly reduce and is independent of the reduce in average light intensity.

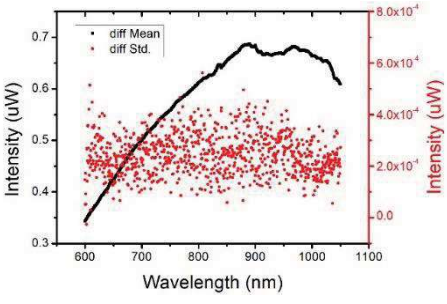


Fig. 5. The difference between the average value (black square) and the average standard deviation (red circle) of the light source and the LMR platform

Furthermore, the comparison of the average standard deviation for the light source and the platform is shown in Fig. 6. The average standard deviation of the LMR platform is distributed from  $1.0 \times 10^{-4} \mu W$  to  $4.0 \times 10^{-4} \mu W$  and the average is about  $2.0 \times 10^{-4}$  µW. The average standard deviation of the light source is distributed from  $2.0\times10^{-4}~\mu\mathrm{W}$  to  $8.0\times10^{-4}~\mu\mathrm{W}$  and the average is about  $5.0 \times 10^{-4} \,\mu\text{W}$ . The former is about 0.4 times the latter. However, the optical power intensity reduced to 6.6% (maximum) and (minimum), with a median value of 4.7%. In short, when the optical power intensity reduces significantly to 4.7%, the average standard deviation drops slightly to 40% (0.4 times). Compared with the same wavelength, a stronger light source intensity causes a larger average standard deviation. However, according to the measurement uncertainty ratio, defined as the average standard deviation divided by the average optical intensity (std./mean %), it is observed that the stronger the light, the lower the uncertainty ratio. For example, the uncertainty ratios are 0.03% in Fig.2 and 0.8% in Fig.3. If the average optical intensity is regarded as the signal, and the average standard deviation is regarded as the noise, the higher the signal-to-noise ratio, the better the measurement quality.

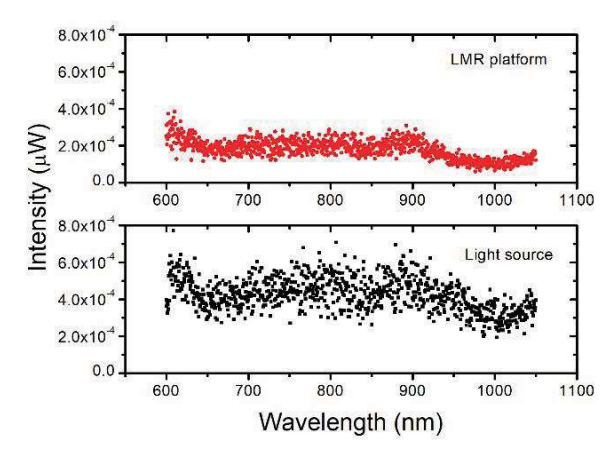


Fig. 6. The distribution of average standard deviation relative to LMR platform (top) and Light source (bottom)

#### 3.3 Uncertainty for the LMR sensor

With different concentrations of glycerol solutions from 0% to 100%, increasing by 20% each time, the refractive indexes (RIs) were

measured as 1.3333, 1.3562, 1.3822, 1.4115, 1.4380, 1.4700, respectively. The definition of RI is the ratio of the velocity of light in a vacuum to its velocity in a specified medium. The relationship between concentration and RI is shown in Fig. 7. It can be found that the higher the concentration of glycerol, the higher RI will be. The linear fitting results give a slope of 0.00137 and intercept of 1.3297 with  $R^2$  of 0.997, as shown in the dash red line in Fig. 7. Because the minimum scale of the refractometer is 0.001 RIU, the error can be set as  $\pm$ 0.0005 RIU. The data recorded at 80% is enlarged to show the error bar of the refractive index, which is illustrated by the inlet in Fig. 7.

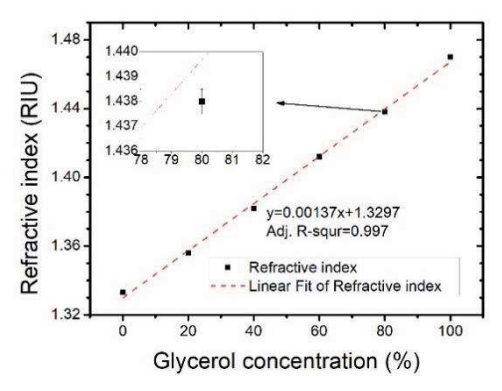


Fig. 7. The correlation and linear fitting of glycerol concentration and refractive index. The inlet is the data of 80% with an error bar

The ITO glass sensor was put on the LMR platform without dripping any substance. The light intensity in the air, the initial power  $P_{\theta}$ , was recorded by the spectrometer. Then, the analyte, solutions of different glycerol concentrations, was dropped on the sensor and the light intensity, the transmitted power, was recorded as  $P_I$ . The  $P_I$  was normalized to  $P_{\theta}$  to get the transmission. The lowest transmission was the resonance point, and the LMR wavelength could be obtained. The measurement was repeated 10 times for each analyte, with an interval of 30 seconds each time. The total period of an analyte was 300 seconds.

The measured transmission spectra are shown in Fig. 8. The points at which the curve dips are the LMR wavelength. Upon increasing the concentration of the glycerol solution, the resonance wavelength shows a red-shift, which means the LMR wavelength is getting longer. The measurement results are consistent with

other documents [8, 17, 18]. The mechanism of red-shift is mainly that the higher the refractive index of the analyte (n), the lower the equivalent wavelength ( $\lambda$ /n). Therefore, a longer wavelength is required to achieve the conditions for LMR. When wavelengths in the transmission spectrum reach a certain length, a sharp loss of energy occurs. The initial resonance wavelength is 881.95 nm for pure water; there is a red-shift to 960.75 nm for pure glycerol. The total shift in the LMR wavelength is 78.80 nm. The transmission also becomes lower and obvious, which decreases from 0.7087 to 0.3558, according to the increase in the RI of an analyte.

The measurement results of all LMR points are organized in Table 1, where  $\lambda_{\mu}$  is the average value of the LMR wavelength, and  $\lambda_{2s}$  is twice the average standard deviation of  $\lambda_{\mu}$ ; while  $T_{\mu}$  is the average value of the LMR transmission, and T<sub>2s</sub> is twice the average standard deviation of  $T_{\mu}$ . In the uncertainty measurement estimation, the expanded coefficient k=2 is applied, which indicates the 95% confidence level for the LMR sensor platform. In the case of RI 1.4380, both the average LMR wavelength of 933.55 nm and the average transmission of 0.4320 increase normally. The uncertainties for the LMR wavelength of 0.18 nm and transmission of 0.0099 are the lowest ones in the table. This could be a random effect, which could be eliminated by more measurements. To summarize the estimation in more detail, the measurement uncertainty of LMR wavelength and LMR transmission are taken respectively to be 0.43 nm and 0.0289 under the confidence level of 95%, which demonstrates the performance of the LMR senor platform.

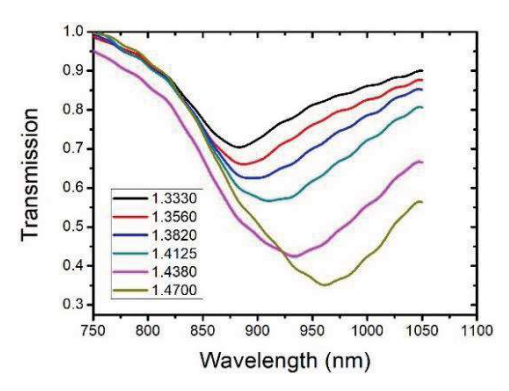


Fig. 8. The transmission spectra for glycerol solution with RI from 1.3330 to 1.4700

Table 1. Average and uncertainty of LMR measurement

Analyte (RI)	λ <sub>μ</sub> (nm)	$\lambda_{2s}(nm)$	$T_{\mu}$	T <sub>2s</sub>
1.3330	881.95	0.38	0.7087	0.0074
1.3560	886.45	0.23	0.6551	0.0289
1.3820	891.21	0.40	0.6266	0.0221
1.4125	910.25	0.43	0.5695	0.0205
1.4380	933.55	0.18	0.4230	0.0099
1.4700	960.75	0.22	0.3558	0.0128

#### IV. CONCLUSIONS

The measurement uncertainty evaluation of Type A is applied for the sensing system of the LMR sensor platform. The system consists of a light source, an LMR sensor, two optical fiber patchcords, and an optical spectrometer. The light source, the LMR platform, and the LMR sensor are experimentally evaluated utilizing the specification document of measurement uncertainty here. Comparing the different wavelengths, the spectrum of a light source with larger intensity will not produce a larger average standard deviation. When comparing cases with the same wavelengths, a light source with stronger intensity will cause a larger average standard deviation. The stronger the intensity of the light, the lower the uncertainty ratio. The performance of the LMR sensor platform is first carried out by examining measurement uncertainty. The LMR wavelength and the transmission are 0.43 nm and respectively, under the confidence level of 95%. As far as we know, this is the first study on the uncertainty measurement of LMR sensors. Furthermore, the methodology of the LMR sensing system opens the possibility to improve the measurement precision and raise the confidence level. The proposed estimation method could be applied to express the measurement results and confidence level objectively and to solve the problem of dynamic balance measurement for biomolecules.

#### REFERENCES

[1] Taha B. A. et al., "Comprehensive Review

- Tapered Optical Fiber Configurations for Sensing Application: Trend and Challenges," *Biosensors*, vol. 11, no. 8, pp. 253, 2021.
- [2] Takemura K., "Surface Plasmon Resonance (SPR)- and Localized SPR (LSPR)-Based Virus Sensing Systems: Optical Vibration of Nano- and Micro-Metallic Materials for the Development of Next-Generation Virus Detection Technology," *Biosensors*, vol. 11, no. 8, pp. 250, 2021.
- [3] Kazzy M. El *et al.*, "An Overview of Artificial Olfaction Systems with a Focus on Surface Plasmon Resonance for the Analysis of Volatile Organic Compounds," *Biosensors*, vol. 11, no. 8, pp. 244, 2021.
- [4] Wang Q., Jiang X., Niu L.-Y., and Fan X.-C., "Enhanced sensitivity of bimetallic optical fiber SPR sensor based on MoS2 nanosheets," *Optics and Lasers in Engineering*, vol. 128, pp. 105997, 2020.
- [5] Zhao Y., Gan S., Zhang G., and Dai X., "High sensitivity refractive index sensor based on surface plasmon resonance with topological insulator," *Results in Physics*, vol. 14, pp. 102477, 2019.
- [6] Nasirifar R., Danaie M., and Dideban A., "Dual channel optical fiber refractive index sensor based on surface plasmon resonance," *Optik*, vol. 186, pp. 194-204, 2019.
- [7] Marciniak M., Grzegorzewski J., and Szustakowski M., "Analysis of lossy mode cut-off conditions in planar waveguides with semiconductor guiding layer," *IEE Proceedings J-Optoelectronics*, vol. 140, no. 4, pp. 247-252, 1993.
- [8] Arregui F. J. *et al.*, "Fiber-optic Lossy Mode Resonance Sensors," *Procedia Engineering*, vol. 87, pp. 3-8, 2014.
- [9] Ascorbe J., Corres J. M., Matias I. R., and Arregui F. J., "High sensitivity humidity sensor based on cladding-etched optical fiber and lossy mode resonances," *Sensors and Actuators B: Chemical*, vol. 233, pp. 7-16, 2016.
- [10] Elosúa C. *et al.*, "Lossy mode resonance optical fiber sensor to detect organic vapors," *Sensors and Actuators B: Chemical*, vol. 187, pp. 65-71, 2013.
- [11] Zamarreño C. R., Hernáez M., Del Villar I.,

- Matías I. R., and Arregui F. J., "Optical fiber pH sensor based on lossy-mode resonances by means of thin polymeric coatings," *Sensors and Actuators B: Chemical*, vol. 155, no. 1, pp. 290-297, 2011.
- [12] Zubiate P., Zamarreño C. R., Del Villar I., I Matias. R., and Arregui F. J., "Tunable optical fiber pH sensors based on TE and TM Lossy Mode Resonances (LMRs)," *Sensors and Actuators B: Chemical*, vol. 231, pp. 484-490, 2016.
- [13] Socorro A. B., Corres J. M., Del Villar I., F. J. Arregui, and Matias I. R., "Fiber-optic biosensor based on lossy mode resonances," *Sensors and Actuators B: Chemical*, vol. 174, pp. 263-269, 2012.
- [14] Zamarreño C. R. *et al.*, "Single strand DNA detection by means of lossy mode resonance-based optical fiber devices," in *2016 IEEE SENSORS*, pp. 1-3, 2016.
- [15] Zubiate P., Zamarreño C. R., Sánchez P., Matias I. R., and Arregui F. J., "High sensitive and selective C-reactive protein detection by means of lossy mode resonance based optical fiber devices," *Biosensors and Bioelectronics*, vol. 93, no. 15 Supplement C, pp. 176-181, 2017.
- [16] Zamarreño C. R. et al., "Route Towards a Label-free Optical Waveguide Sensing Platform Based on Lossy Mode Resonances," Sensors & Transducers Journal, vol. 11, no. 138, 2019.
- [17] Fuentes O., Corres J. M., Domínguez I.,

- Villar I. d., and Matias I. R., "Simultaneous Measurement of Refractive Index and Temperature using LMR on planar waveguide," in 2020 IEEE Sensors, 2020, pp. 1-4
- [18] Fuentes O., Del Villar I., Corres J. M., and Matias I. R., "Lossy mode resonance sensors based on lateral light incidence in nanocoated planar waveguides," *Scientific reports*, vol. 9, no. 1, pp. 1-10, 2019.
- [19] I. O. f. Standardization, Uncertainty of measurement-Part 3: Guide to the expression of uncertainty in measurement (GUM: 1995). ISO, 2008.
- [20] Lin Y.-C., Chen L.-Y., and Chiu F.-C., "Lossy Mode Resonance-Based Glucose Sensor with High-κ Dielectric Film," *Crystals*, vol. 9, no. 9, p. 450, 2019.
- [21] Karazi S. M., Ahad I. U., and Benyounis K. Y., "Laser Micromachining for Transparent Materials," in *Reference Module in Materials Science and Materials Engineering*: Elsevier, 2017.
- [22] Rubin M., "Optical properties of soda lime silica glasses," *Solar energy materials*, vol. 12, no. 4, pp. 275-288, 1985.
- [23] Paliwal N. and John J., "Lossy Mode Resonance Based Fiber Optic Sensors," in Fiber Optic Sensors: Current Status and Future Possibilities, I. R. Matias, S. Ikezawa, and J. Corres, Eds. Cham: Springer International Publishing, 2017, pp. 31-50.

Yu-Cheng Lin Analysis of Lossy Mode Resonance Sensing System Using Measurement Uncertainty of Type A